Published in final edited form as:
J Immunol. 2014 December 15; 193(12): 6070–6080. doi:10.4049/jimmunol.1400654.

Infiltrating regulatory B-cells control neuroinflammation following viral brain infection

Manohar B. Mutnal[*], **Shuxian Hu**[*], **Scott J. Schachtele**[*], and **James R. Lokensgard**[*†]

[*†]Neuroimmunology Laboratory, Center for Infectious Diseases and Microbiology Translational Research, Department of Medicine, University of Minnesota, Minneapolis MN 55455

Abstract

Previous studies have demonstrated the existence of a subset of B lymphocytes, regulatory B-cells (Bregs), which modulate immune function. Here, *in vivo* and *in vitro* experiments were undertaken to elucidate the role of these Bregs in controlling neuroinflammation following viral brain infection. We used multi-color flow cytometry to phenotype lymphocyte subpopulations infiltrating the brain, along with *in vitro* co-cultures to assess their anti-inflammatory and immunoregulatory roles. This distinctive subset of $CD19^{+}CD1d^{hi}CD5^{+}$ B-cells was found to infiltrate the brains of chronically infected animals, reaching highest levels at the latest time point tested (30 d p.i.). B-cell-deficient $Jh^{-/-}$ mice were found to develop exacerbated neuroimmune responses as measured by enhanced accumulation and/or retention of $CD8^{+}$ T-cells within the brain, as well as increased levels of microglial activation (MHC class II). Conversely, levels of $Foxp3^{+}$ regulatory T-cells (Tregs) were found to be significantly lower in $Jh^{-/-}$ mice when compared to wild-type (Wt) animals. Further experiments showed that *in vitro* generated IL-10-secreting regulatory B-cells (B10) were able to inhibit cytokine responses from microglia following stimulation with viral antigens. These *in vitro* generated B10 cells were also found to promote proliferation of regulatory T-cells in co-culture studies. Finally, gain of function experiments demonstrated that reconstitution of Wt B-cells into $Jh^{-/-}$ mice restored neuroimmune responses to levels exhibited by infected Wt mice. Taken together, these results demonstrate that regulatory B-cells modulate T lymphocyte as well as microglial cell responses within the infected brain and promote $CD4^{+}Foxp3^{+}$ T-cell proliferation *in vitro*.

Introduction

The central nervous system (CNS) is a target for acute viral infection, as well as a reservoir of latent and persisting viruses (1, 2). The prevailing paradigm has been that the inert immunological status of the CNS parenchyma is maintained through exclusion of key components of the immune system. However, it is now known that systemic T lymphocytes (3) normally transit into the CNS to participate in immune surveillance (4). Proinflammatory cytokines, chemokines, and other mediators produced by resident glial cells, both astrocytes and microglia, induce activation and recruitment of immune cells in response to viral infection (5–8). However, a balance is required between the neuroimmune responses that are

[#]Corresponding author: James R. Lokensgard, University of Minnesota, 3-220 LRB/MTRF, 2001 6th Street S.E., Minneapolis, MN 55455, USA, Tel: (612)-626-9914, Fax: (612)-626-9924, loken006@umn.edu.

necessary to deal with invading pathogens and those that prevent these responses from harming surrounding brain tissue. Long-term persistence of immune cells that infiltrate the CNS in several viral infections demonstrates that inflammation needs to be controlled to prevent immune-driven pathology, through either native or external anti-inflammatory mechanisms. Various regulatory cell types and anti-inflammatory mediators have been shown to play critical roles in counteracting these overzealous neuroinflammatory responses and preventing immune-mediated neuropathology (9–11).

A number of anti-inflammatory mechanisms have been demonstrated to control excess neuroinflammation including the infiltration of inflammation-dampening regulatory T-cells (Tregs) (12). Interleukin (IL)-10 is the prototypical anti-inflammatory cytokine that suppresses cellular immunity and inhibits synthesis and release of proinflammatory mediators from activated microglia, (13, 14). Tregs have been identified as a predominant source of IL-10, but studies have shown that this cytokine can also be produced by many other types of immune cells including B-cells (15–17).

B lymphocytes have been traditionally considered antigen-presenting and antibody-producing cells. However, a number of studies in recent years have demonstrated the existence of a regulatory subset of B-cells (Bregs) that exhibit immunosuppressive functions (reviewed in (18). An early study by Fillatreau et al. (19), using a chimeric model where B-cells were specifically deleted of IL-10 production, demonstrated that these cells inhibited immune-mediated pathology in murine experimental autoimmune encephalomyelitis (EAE). Further studies went on to reveal that Bregs play important roles in control of immunopathology during autoimmune diseases (16), cancer (20), and organ transplantation (21). Breg cells have also been shown to modulate immune responses and immunopathology in infectious diseases (22, 23). Different phenotypes of Bregs have been described. These cells have been detected within splenic marginal zone (MZ) populations (24). IL-10 producing B-cells are found in the spleens of naive mice at low frequencies (1–5%), where they represent a subset of the $CD19^{+}CD1d^{hi}CD5^{+}$ B-cell subpopulation (15, 16, 25). These $CD1d^{hi}CD5^{+}$ B-cells were found to be more enriched for IL-10–producing cells (9%–15%) than other B-cell subsets. Similar IL-10-producing B-cell subsets have been identified in healthy and autoimmune individuals. The capacity of human and mouse Breg cells to express IL-10 is central to their negative regulation of inflammation, autoimmunity, and adaptive as well as innate immune responses (26–29). B-cell expression of cytoplasmic IL-10 protein parallels both their expression of IL-10 transcripts and secretion of IL-10, as measured by ELISA (26–29). In this manuscript we use the term Breg to identify cells expressing the $CD19^{+}CD1d^{hi}CD5^{+}$ surface markers, while the term B10 cells is used to describe B-lineage cells known to produce IL-10.

Our previous studies have demonstrated that viral brain infection with murine cytomegalovirus (MCMV) triggers accumulation and long-term persistence of both T lymphocyte- and B lymphocyte-lineage cells within the brain (30, 31). While $CD8^{+}$ T-cells were found to be required for viral clearance and control of brain infection (32), persisting B-lineage cells were found to produce MCMV-specific antibodies and played a significant role in controlling spread of reactivated virus (31). In the present study, we assessed the

presence of $CD19^{+}CD1d^{hi}CD5^{+}$ Breg cells within the infected brain and investigated their anti-inflammatory and immunoregulatory roles.

Materials and Methods

Ethical statement

This study was carried out in strict accordance with recommendations in the Guide for the Care and Use of Laboratory Animals of the National Institutes of Health. The protocol was approved by the Institutional Animal Care and Use Committee (Protocol Number: 1105A99534) of the University of Minnesota. All surgery was performed under Ketamine anesthesia, and all efforts were made to minimize suffering.

Virus and animals—RM461, a MCMV expressing *Escherichia coli* β-galactosidase under the control of the human ie1/ie2 promoter/enhancer (33) was kindly provided by Edward S. Mocarski. The virus was maintained by passage in weanling female BALB/c mice. Salivary gland-passed virus was then grown in NIH 3T3 cells for 2 passages, which minimized any carryover of salivary gland tissue. Infected 3T3 cultures were harvested at 80% to 100% cytopathic effect and subjected to three freeze–thaw cycles. Cellular debris was removed by centrifugation (1000 ×*g*) at 4 °C, and the virus was pelleted through a 35% sucrose cushion (in Tris-buffered saline [50 mM Tris–HCl, 150 mM NaCl, pH 7.4]) at 23,000 ×*g* for 2 h at 4 °C. The pellet was resuspended in Tris buffered saline containing heat-inactivated fetal bovine serum (FBS, Sigma, St. Louis, MO). Viral stock titers were determined on 3T3 cells as 50% tissue culture infective doses ($TCID_{50}$) per milliliter. Six to eight weeks old BALB/c mice were obtained from Charles River Laboratories (Wilmington, MA), while B-cell deficient mice ($Jh^{-/-}$) were a kind gift from Dr. Steven McSorley (University of California, Davis) (34, 35). In $Jh^{-/-}$ mice, T-lymphocyte development proceeds normally, based on surface phenotype and quantity of cells in the spleen; splenic lymphocytes are enriched for T-cells due to B-cell deficiency (35). IL-10-GFP knock-in mice (B6.129S6-Il10tm1Flv/J) (28) were kindly provided by Dr. Sing Sing Way (Cincinnati Children's Hospital, Cincinnati, OH). $Foxp3^{EGFP}$ mice (B6.Cg-Foxp3tm2Tch/J) were obtained from Jackson Laboratories, Bar Harbor, ME.

Intracerebroventricular infection—Infection of mice with MCMV was performed as previously described (36). Briefly, female mice (6–8 week old) were anesthetized using a combination of Ketamine and Xylazine (100 mg and 10 mg/kg body weight, respectively) and immobilized on a small animal stereotactic instrument equipped with a Cunningham mouse adapter (Stoelting Co., Wood Dale, IL). The skin and underlying connective tissue were reflected to expose reference sutures (sagittal and coronal) on the skull. The sagittal plane was adjusted such that the bregma and lambda were positioned at the same coordinates on the vertical plane. Virulent, salivary gland-passaged MCMV RM461 (1.5×10^5 $TCID_{50}$ units in 10 μl), was injected into the right lateral ventricle at 0.9 mm lateral, 0.5 mm caudal to the bregma and 3.0 mm ventral to the skull surface using a Hamilton syringe (10 μl) fitted to a 27 G needle. The injection was delivered over a period of 3–5 min. The opening in the skull was sealed with bone wax and the skin was closed using 9 mm wound clips (Stoelting Co., Wood Dale, IL).

Isolation of brain leukocytes and flow cytometry analysis—Leukocytes were isolated from MCMV-infected murine brains using a previously described procedure with minor modifications (37–40). In brief, brain tissues harvested from four to six animals were minced finely in RPMI 1640 (2 g/L D-glucose and 10 mM HEPES, Sigma) and digested in 0.0625% trypsin (in Ca/Mg-free HBSS, Sigma) at room temperature for 20 min. Single cell preparations from infected brains were resuspended in 30% Percoll (Sigma) and banded on a 70% Percoll cushion at 900 × g for 30 min at 15°C. Brain leukocytes obtained from the 30–70% Percoll interface were treated with Fc block (anti-CD32/CD16 in the form of 2.4G2 hybridoma culture supernatant with 2% normal rat and 2% normal mouse serum) to inhibit nonspecific Ab binding and were stained with anti-mouse immune cell surface markers for 45 min at 4°C and analyzed by flowcytometry. Bregs from brain-infiltrating leukocytes were identified by flowcytometry using Breg staining kit from BioLegend, San Diego, CA. Control isotype Abs were used for all isotype and fluorochrome combinations to assess nonspecific Ab binding. Live leukocytes were gated using forward scatter and side scatter parameters on a BD FACSCanto flow cytometer (BD Biosciences, San Jose, CA). Data was analyzed using FlowJo software (TreeStar, Ashland, OR).

B-cell isolation and stimulation—We employed two different protocols to generate B10 cells *in vitro.* B10 cells generated with the first protocol were used in microglia and Breg co-culture studies. In these experiments, B10 cells were prepared following published protocols with minor modifications. Briefly, $CD19^+$ lymphocytes from IL-10-GFP knock-in mice were enriched by negative selection using a $CD19^+$ cell purification kit, as per the manufacturer's instructions (R&D Systems, Minneapolis, MN). For preparation of B10 cells, 1×10^6 purified B-cells were cultured with agonistic CD40 mAB (1 μg/ml, Miltenyi Biotec, Auburn, CA) for 48 h. For the last 5 h, cells were treated with LPS (10 μg/ml, Sigma), PMA and Ionomycin (eBioscience San Diego, CA). Post-stimulation, cells were subjected to FACS using FACSAria (BD Biosciences). GFP expression indicated that the cells were IL-10 competent. Post-sorting, the B10 cells were co-cultured with microglial cells at a ratio of 5:1, respectively. Microglial cells were stimulated with MCMV with an MOI of 5. Culture supernatants were collected after 24 h from the various treatment groups to assess cytokine production by ELISA. Additional protocols for generating B10 cells that avoid the use of LPS have been described (41). We employed B10 cells generated through this protocol in B10 and $CD4^+$ T-cells co-culture studies at a ratio of 1:1. Briefly, splenic $CD19^+$ lymphocytes from BALB/c mice were enriched by negative selection using a $CD19^+$ cell purification kit, as per the manufacturer's instructions (R&D Systems, Minneapolis, MN). Purity of the $CD19^+$ cells was found to be >98.8%. For preparation of B10 cells, purified B-cells were cultured with IL-4 (10 ng/ml, eBioscience San Diego CA), with agonistic CD40 mAB (1 μg/ml, Miltenyi Biotec, Auburn CA) and BAFF (20 ng/ml, eBioscience) for 4 d. Approximately 45% of the B10 cells thus produced were found to be positive for intracellular IL-10, as measured by flow cytometry. Positive control cells, designated iTregs in Fig 6, were generated using previously published protocols with minor modifications (42). Briefly, $CD4^+$ T-cells were isolated from spleens of $Foxp3^{EGFP}$ reporter mice by negative selection, according to manufacturer's instructions (R&D Systems). Cells were cultured at a density of 2×10^6 cells/ml in 24-well plates for 5 days in RPMI medium supplemented with plate-bound anti-CD28 (1 μg/ml), anti-CD3 (10 μg/ml) (Bio X cell, West

Lebanon, NH), IL-2 (10 ng/ml) and TGF-β1 (5 ng/ml) (eBioscience) to induce differentiation of $Foxp3^+$ $CD4^+$ T regulatory cells.

Murine microglial cell cultures—Microglial cells were isolated from cerebral cortices of 1-day-old mice as previously described (43, 44). Briefly, after a 30-min trypsinization (0.25%), dispersed cortical cells were plated in Falcon 75 cm2 culture flasks in DMEM (Sigma) containing 10% heat inactivated fetal bovine serum (FBS; Hyclone, Logan UT), penicillin (100 U/ml) and streptomycin (100 μg/ml) (Sigma). Medium was changed at days 1 and 4 after plating. On day 8 of culture, flasks were shaken for 20 min in an orbital shaker at 180–200 rpm to remove oligodendrocytes. On days 12–14 of culture, floating microglia were harvested by gentle shaking and seeded into 24- or 48-well culture plates ($1–2 \times 10^4$ cells/well) and washed after 60 min. Adherent microglial cells were ≥ 95% pure, as determined by MAC-1 (microglial cell marker; Roche, Indianapolis, IN) and glial fibrillary acidic protein (GFAP-marker for astrocytes; Sigma) antibody staining (45, 46). All *in vitro* experiments used primary cell types which were genetically matched.

Adoptive transfer—Spleens from MCMV primed (1×10^5 $TCID_{50}$/mouse, i.p. injection) donor animals were collected aseptically at 7 d post-priming. Single cell suspensions of immunocytes were depleted of RBC by treatment with 0.87% ammonium chloride, washed twice, and cell viability was confirmed using trypan blue. $CD19^+$ lymphocytes were enriched by negative selection using a $CD19^+$ cell purification kit, as per the manufacturer's instructions (R&D systems). Immune cells were transferred (5×10^6 cells/mouse) via tail vein 1 d prior to infection with MCMV into syngenic ($Jh^{-/-}$) recipients.

Results

Bregs persist within chronically-infected brains

MCMV brain infection models have provided tremendous insights into viral neuropathogenesis and the role of immune responses in controlling infection (32, 47). In previous studies using our murine CMV brain infection model, we have identified brain-infiltrating B lymphocyte lineage cells, identified as $CD19^+$ B-cells and $CD138^+$ plasma cells (31). In this study, we also detected a B-cell subset expressing $CD19^+CD1d^{hi}CD5^+$ phenotype which possesses negative regulatory functions within the brains of MCMV-infected mice. We used a multi-color flow cytometry approach to phenotype lymphocyte subpopulations infiltrating the brain at various time points p.i. Brain-infiltrating mononuclear cells were isolated on a Percoll gradient as described in the methods. These isolated cells were subsequently immunostained for expression of the markers CD45, CD11b, CD3, CD19, CD1d and CD5. Breg cells expressing the $CD19^+CD1d^{hi}CD5^+$ cell surface markers were identified among the $CD45^{hi}$ population, which represent cells of lymphoid origin. At 7 d p.i., 2.25% of the cells among the $CD19^+$ population were reactive to $CD1d^{hi}CD5^+$ and this subset was found to increase to 5.19% and 18.06% at 14 and 30 d p.i., respectively (Fig 1A). The absolute number of $CD19^+CD1d^{hi}CD5^+$ cells was also determined. Presence of Breg cells was apparent within the infected brain starting at 7 d p.i. ($3.3 \pm 1.0 \times 10^4$), they were present at 14 d p.i. ($1.5 \pm 0.4 \times 10^5$), and persisted at least until 30 d p.i. ($1.7 \pm 0.5 \times 10^5$). There was a significant increase in the accumulation of Breg cells

at both 14 and 30 d p.i. when compared to 7 d p.i. ($1.5 \pm 0.4 \times 10^5$ and $1.7 \pm 0.5 \times 10^5$ versus $3.3 \pm 1.0 \times 10^4$, respectively, $p < 0.05$ Student's *t* test) (Fig 1B). We determined the percentage of $CD19^+CD1d^{hi}CD5^+$ expressing cells at the indicated times p.i. from 3 independent experiments. Pooled data presented show that at 30 d p.i. there was a significant increase in the percentage of these cells infiltrating the brain when compared to 7 d p.i. ($16.94 \pm 1.2\%$ versus $5.9 \pm 4.8\%$, $p < 0.05$ Student's *t* test) (Fig 1C). In order to investigate the infiltration kinetics of Bregs ($CD1dhiCD5^+$) relative to total B-cells, we determined the absolute number of $CD19^+$ cells among the total infiltrating CD45hi population (i.e., including $CD3^+$ cells). The presence of $CD19^+$ cells was observed as early as 7 d p.i. and there was a significant increase in their numbers at 14 and 30 d p.i. when compared to 7 d p.i. ($1.6 \pm 0.16 \times 10^5$ and $2.5 \pm 1.1 \times 10^5$ versus $6.0 \pm 1.6 \times 10^4$, respectively, $p < 0.05$ Student's *t* test) (Fig 1D). The absolute number of Bregs ($CD1dhiCD5^+$) within total infiltrating CD45hi population was then determined. We observed that there was a significant increase in the presence of Breg cells at 30 d p.i. when compared to 7 d p.i. ($5.3 \pm 2.7 \times 10^3$ versus $5.1 \pm 2.7 \times 10^2$, respectively, $p < 0.05$ Student's *t* test) (Fig 1E).

B-cell deficiency alters long-term T-cell persistence within the infected brain

Previous studies from our laboratory have shown that $CD8^+$ T-cells are essential in resolving MCMV brain infection, through a perforin-mediated mechanism (32). In subsequent studies we showed that memory $CD8^+$ T-cells persisting in the brain drive chronic microglial activation through an interferon (IFN)-γ-dependent manner, despite the absence of active viral replication, suggesting that long-term persisting $CD8^+$ T-cells may contribute to immunopathology in the CNS (30). In the current study, we found a correlation between the absence of B-cells and an increased presence of $CD8^+$ T-cells along with decreased $CD4^+$ T-cell numbers within infected brains. MCMV-infected Wt as well as B-cell deficient ($Jh^{-/-}$) mice were analyzed for a number of neuroimmune responses which included phenotyping of the brain-infiltrating cell populations. The representative contour plots shown in Fig. 2 were obtained from isolated brain infiltrating cells, gated on $CD45^{hi}$, and subsequently analyzed for the presence of $CD4^+$ and $CD8^+$ T-cells (Fig 2A). A significant increase in the absolute number of infiltrating $CD8^+$ T-cells was observed in the $Jh^{-/-}$ mice ($1.6 \pm 0.2 \times 10^6$ versus $1.1 \pm 0.11 \times 10^6$, $p < 0.05$), when compared to Wt animals (Fig 2B). On the contrary, a significant decrease in the absolute numbers of infiltrating $CD4^+$ T-cells was observed in these animals ($3.6 \pm 0.1 \times 10^5$ versus $1.1 \pm 0.3 \times 10^5$, $p < 0.05$) (Fig 2B). Analysis of pooled data from 3 independent experiments showed a significantly elevated percentage of $CD8^+$ T-cells in the brains of B-cell deficient mice when compared to Wt controls, ($80.9 \pm 1.2\%$ versus $69.1 \pm 0.9\%$, respectively, $p < 0.05$ Student's *t* test) (Fig 2C). Additionally, the $CD4^+$ T-cell percentage was also found to be significantly lower in $Jh^{-/-}$ mice when compared with Wt mice ($13.9 \pm 0.4\%$ versus $20.4 \pm 0.9\%$, $p < 0.05$ Student's *t* test) (Fig 2C). We also performed flow cytometry assays on single cell suspensions prepared from draining lymph nodes (dLN) of MCMV-infected Wt and $Jh^{-/-}$ animals at 30 d p.i. Interestingly, impaired T-cell recruitment into the CNS during B-cell deficiency was observed despite elevated levels of T-cells within the draining lymph nodes of $Jh^{-/-}$ mice. The flow cytometric analysis shown in Fig 2D indicated that there were elevated levels of both $CD4^+$ and $CD8^+$ T-cells in the dLN of $Jh^{-/-}$ mice at 30 d p.i. We determined absolute numbers and percentages of both $CD4^+$ and $CD8^+$ T-cells in the periphery (dLN) of Wt and Jh−/− animals and observed that

there was a significant increase in the total number and percentage of $CD4^+$ T-cells $Jh^{-/-}$ mice when compared to Wt ($3.5 \pm 0.1 \times 10^6$ versus $2.8 \pm 0.3 \times 10^6$ and $68.6 \pm 3.5\%$ versus $47.3 \pm 6.5\%$, respectively, $p < 0.05$). On the contrary, we observed there was no significant increase in the total number of $CD8^+$ T-cells in dLN of $Jh^{-/-}$ animals when compared to Wt mice at 30 d p.i, however, statistical analysis of percentage data showed a significant increase in $CD8^+$ T-cells in the $Jh^{-/-}$ animals in the dLN at 30 d p.i., when compared Wt mice. ($18.0 \pm 0.5\%$ versus $24.6 \pm 2.3\%$, $p < 0.05$) (Figs 2E and F).

Frequencies of $CD4^+Foxp3^+$ regulatory T-cells were reduced in the brains of $Jh^{-/-}$ mice

Tregs are critical for normal functioning immune responses by providing a mechanism to maintain self-tolerance, while still allowing for protective responses against microbes. Several studies have investigated the role of Treg cells, defined as $CD4^+Foxp3^+$, in regulation of immune responses to infectious diseases (48–50). Since we observed a significant decrease in the presence of $CD4^+$ T-cells within the brains of $Jh^{-/-}$ mice at 30 d p.i., despite higher levels in the dLN, we next examined whether other $CD4^+$ T-cell subsets, particularly anti-inflammatory cells such as regulatory T-cells, were altered. In these experiments we assessed the presence of regulatory T-cells in the brains of chronically infected Wt and $Jh^{-/-}$ mice. At 30 d p.i., we collected brain tissues and processed them for isolation of infiltrating mononuclear cells. The cells were subjected to staining with cell surface markers CD45, CD11b, and CD4 followed by intranuclear staining for Foxp3. Representative contour plots from Wt and $Jh^{-/-}$ mice for $CD4^+Foxp3^+$ T-cells, from brain and dLN, that were gated from the $CD45^{hi}$ cell population are shown (Fig 3A). Analysis of pooled data showed a significant decrease in the absolute numbers of $CD4^+Foxp3^+$ T-cells recruitment within the infected brains in $Jh^{-/-}$ mice ($5.1 \pm 1.1 \times 10^4$ versus $3.0 \pm 0.6 \times 10^4$, $p < 0.05$) (Fig 3B). Pooled data from 3 independent experiments also showed a significant decrease in the percentage of $CD4^+Foxp3^+$ T-cells in $Jh^{-/-}$ mice when compared to MCMV infected Wt animals, $3.5 \pm 0.5\%$ versus $8.77 \pm 0.5\%$, $p < 0.05$ Student's *t* test (Fig 3C). We also determined the percentage and absolute numbers for Tregs in the dLN from Wt and $Jh^{-/-}$ animals at 30 d p.i., and the data presented show that there were no significant differences in the presence of Tregs in the dLN of $Jh^{-/-}$ mice when compared with Wt animals (Figs 3D and E).

Increased $CD8^+$ T-cell presence and reduced regulatory T-cells promote enhanced chronic microglial activation with B-cell deficiency

To compare chronic activation of brain-resident microglia between MCMV-infected Wt versus $Jh^{-/-}$ animals, these cells were assessed by first gating on the $CD45^{int}CD11b^+$ population, isolated at 30 d p.i., followed by evaluation of MHC class II, CD40, and CD86 expression using flow cytometry. Representative histogram overlays demonstrate a shift in the expression levels of MHC class II on microglia from $Jh^{-/-}$ mice (dotted line) when compared with Wt animals (solid line), (Fig 4A). This shift indicated an increased level of microglial activation within the brains of B-cell-deficient animals. In addition, the mean fluorescence intensity (MFI) of MHC II expression was also measured between groups and was found to be significantly higher among microglia isolated from $Jh^{-/-}$ mice ($1.0 \pm 0.1 \times 10^4$ versus $1.9 \pm 0.1 \times 10^4$, $p < 0.01$ Student's *t* test) (Fig 4B). CD40 and CD86 expression on microglial cells was also assessed and the flow cytometry histogram data showed

increased expression of these molecules on microglia derived from $Jh^{-/-}$ animals at 30 d p.i. (Fig 4C). Statistical analysis of percent expression of CD40 and CD86 molecules showed a significant increase in their expression on cells isolated from $Jh^{-/-}$ mice when compared with Wt animals (10.2 ± 0.9% versus 5.8 ± 0.3% and 26.2 ± 1.0 % versus 17.6 ± 1.0%, respectively, $p < 0.05$ Student's *t* test) (Fig 4D). In addition, mean fluorescence intensity for CD40 and CD86 expression on microglial cells was measured and was found to be significantly higher among those isolated from $Jh^{-/-}$ mice (170 ± 30 versus 380 ± 19 for CD40 and 330 ± 23 versus 540 ± 13 for CD86, $p < 0.05$ Student's *t* test) (Fig 4E).

In-vitro generated B10 cells modulate microglial cell responses through IL-10 production

Previous studies have shown that the anti-inflammatory cytokine IL-10 inhibits secretion of proinflammatory mediators from macrophages (51). In this study, we examined the effect of IL-10, produced by B10 cells, on microglial cells stimulated with MCMV. To evaluate the effects of Bregs on cytokine production by microglia, we focused on the subset of IL-10-producing Bregs, B10 cells, for which we can generate enriched populations *in vitro*. Tumor necrosis factor (TNF)-α levels were quantified from supernatants of purified microglial cell cultures following stimulation with MCMV in either the presence or absence of B10 cells. Fig 5A shows the protocol used for *in vitro* generation of B10 cells from naïve B-cells of MHC-matched IL-10-GFP knock-in donor mice. Representative contour plots of B-cells that were treated with the above protocol and analyzed for GFP^+ cells, indicative of IL-10 synthesis, are shown in Fig 5B. The GFP^+ cells were then enriched by fluorescent activated cell sorting (FACS) and these enriched cells were used in subsequent co-culture experiments. In the first set of experiments, we detected IL-10 production in supernatants from the B10: microglial cell co-cultures. Data demonstrate that IL-10 was produced in the co-culture system that included $CD19^+GFP^+$ cells, but it was not detected when $CD19^+GFP^-$ cells were used to reconstitute the co-cultures (Fig 5C). Further studies using this co-culture system revealed that B10 cells had a suppressive effect on microglial cells that were stimulated with MCMV for 24 h. Microglia which were co-cultured with $CD19^+GFP^+$ B10 cells produced significantly lower levels of TNF-α in response to stimulation with MCMV when compared to microglial cells co-cultured with $CD19^+GFP^-$ cells (Fig 5D). We went on to demonstrate that addition of anti-IL-10 neutralizing antibody to the co-culture system resulted in an abrogation of the suppressive effect of B10 cells on microglia, demonstrating an inhibitory role for B10-produced IL-10 (Fig 5D).

B10 cells promote proliferation of $CD4^+Foxp3^+$ Tregs

Our data show that the absence of B-cells resulted in reduced numbers of Tregs persisting within the brain following viral infection. To address whether B10 cells promote conversion of $CD4^+$ T-cells into Tregs or induce their proliferation, we utilized an *in vitro* generated B10 and $CD4^+$ T-cell co-culture system. B10 cells were generated following the protocol noted in the methods section. To confirm the successful generation of B10 cells using the specified stimulation protocol, we first examined the cells for their ability to produce IL-10 by intracellular staining and flow cytometry. In these experiments, IL-10 production was detected in approximately 47% of the B-cells. Correspondingly, these *in vitro* generated B10 cells were subsequently phenotyped for typical B-cell markers such as IgM^+ (95%), IgD^+ (51%), $IgG1^+$ (66%), $B220^+$ (87%), $CD21^+$ (88%), $CD93^+$ (23%), $CD23^+$ (82%) and $CD19^+$

(84%) prior to their use in co-culture studies. Representative histogram plots show IL-10 producing $CD19^+$ cells as well as the expression of various surface markers following treatment (Fig 6A and B, respectively). These B10 cells were subsequently co-cultured with $CD4^+$ T-cells from $Foxp3^{EGFP+}$ mice for 72 h, followed by analysis of $Foxp3^{EGFP}$ expression using flow cytometry. Representative contour plots shown are from: $CD4^+$ T-cells from non-GFP animals for gating purposes, $CD4^+$ T-cells alone, $CD19^+$: $CD4^+$ T-cell co-cultures, B10: $CD4^+$ T-cell co-cultures, and induced Tregs (iTreg) as a positive control (using a standard protocol to generate iTregs from naïve $CD4^+$ T-cells) (Fig 6C). The ability of B-cells to induce Treg proliferation, both *in vitro* and *in vivo*, has been previously reported (52). In order to differentiate between conversion and proliferation of Tregs we performed intranuclear staining for Ki67 expression in $CD4^+$ T-cells co-cultured with B10 cells. These experiments showed that approximately 8% of the $Foxp3^+$ cells also expressed Ki67, suggesting that the Tregs proliferated in presence of B10 cells. Representative contour plots, gated on $CD4^+$ cells, are shown from $CD4^+$ only, B10:$CD4^+$, and iTregs (Fig. 6D). The amount of $CD4^+Foxp3^+$ T-cells present was found to be significantly higher in B10:$CD4^+$ T-cell co-cultures when compared with the other treatment groups. (11 ± 1.3% ($CD4^+$ only), and 9 ± 1.3% ($CD19^+$:$CD4^+$) versus 27 ± 0.9% (B10:$CD4^+$), $p < 0.01$ Student's *t* test). Data shown in the bar graph are from three independent co-culture experiments (Fig 6E).

Transfer of B-cells into MCMV-infected $Jh^{-/-}$ mice restores T-cell levels within chronically-infected brains

To evaluate the contributions of B-cells in regulating neuroimmune responses during the chronic phase of disease, we went on to perform adoptive transfer experiments. Using this gain-of-function approach, we transferred MCMV-primed $CD19^+$ B-cells, isolated from MHC matched donors, into $Jh^{-/-}$ mice. These B-cell deficient $Jh^{-/-}$ mice received 5×10^6 primed $CD19^+$ B-cells 1 d prior to infection. At 30 days p.i., we harvested brains from Wt, $Jh^{-/-}$, and reconstituted (B-cell AT) mice, and brain-infiltrating leukocytes were purified using a Percoll gradient. These cells were then analyzed by flow cytometry following the appropriate immunostaining. Representative contour plots for $CD4^+$, $CD8^+$ (upper panel) and $CD4^+$ $Foxp3^+$ (lower panel) are shown from the various groups of animals at 30 d p.i. (Fig 7A). Adoptive transfer of B-cells into $Jh^{-/-}$ mice restored the levels of $CD4^+$, $CD8^+$ and $Foxp3^+CD4^+$ T-cells to those observed in infected Wt mice. We determined absolute numbers for $CD4^+$ T-cells ($3.4 \pm 0.7 \times 10^5$ (Wt), $3.2 \pm 0.7 \times 10^5$ ($Jh^{-/-}$ +AT) versus $1.4 \pm 0.4 \times 10^5$ ($Jh^{-/-}$), $p < 0.05$ Student's *t* test), $CD8^+$ T-cells ($1.1 \pm 0.1 \times 10^6$ (Wt), $1.3 \pm 0.4 \times 10^6$ ($Jh^{-/-}$ +AT) versus $1.6 \pm 2.2 \times 10^6$ ($Jh^{-/-}$), $p < 0.05$ Student's *t* test), and $CD4^+Foxp3^+$ T-cells ($4.8 \pm 1.0 \times 10^4$ (Wt), $5.0 \pm 0.9 \times 10^4$ ($Jh^{-/-}$ +AT) versus $2.8 \pm 0.2 \times 10^4$ ($Jh^{-/-}$), $p < 0.05$ Student's *t* test) within the brains of Wt and $Jh^{-/-}$ animals. These data indicated that replenishing B-cells into $Jh^{-/-}$ animals restored neuroimmune responses to levels exhibited by Wt animals (Fig 7B). Similarly, MHC class II expression on microglial cells isolated from $Jh^{-/-}$ mice receiving B-cell transfer was also restored to the levels exhibited by Wt animals. Representative histogram overlays are shown from the various groups of animals (Fig 7C). Mean fluorescence intensity of MHC II expression was also measured among the groups and was found to be significantly higher on microglia isolated from $Jh^{-/-}$ mice (1.1 ±

0.1 ×10^4 (Wt), 1.2 ± 0.1 ×10^4 ($Jh^{-/-}$ +AT) versus 1.9 ± 0.1 ×10^4 ($Jh^{-/-}$), $p < 0.01$ Student's *t* test) (Fig 7D).

Discussion

Neuroimmune responses elicited during CNS infections are critical in controlling viral replication and promoting successful resolution; however, certain aspects of both innate and adaptive responses, if not appropriately regulated, may induce neuropathology. It is clear that excessive production of inflammatory mediators induced during various stages is a primary mechanism responsible for pathogenesis during many viral infections. Therefore, adequate function of the immune regulation arm, mediated by immunosuppressive cytokines and regulatory immune cells, plays a critical role in controlling excess inflammatory responses and their associated damage (53).

In addition to antibody production, specific subsets of B-cells are also known to regulate T-cell- and macrophage-driven immune responses and over the last decade the concept of anti-inflammatory Breg cells has emerged (18). In the present study, our first experiments analyzed the presence of these Breg cells during chronic viral brain infection with MCMV. Results obtained showed that there was a sustained presence of Breg cells within the brains of mice following viral infection. While assessing function we found that B-cell deficient animals developed exacerbated neuroimmune responses, as measured by enhanced accumulation of $CD8^+$ T-cells and increased levels of microglial activation. Additional experiments showed that the absence of B-cells led to a significant reduction in accumulation of regulatory T-cells within the brains of infected $Jh^{-/-}$ mice when compared with Wt animals. Furthermore, *in vitro* generated B10 cells were able to inhibit cytokine responses from MCMV-stimulated microglial cells. We went on to show that these *in vitro* generated B10 cells also promoted proliferation of Foxp3-expressing regulatory T-cells. In the final experiments, adoptive transfer of B-cells into MCMV-infected $Jh^{-/-}$ mice was found to restore T-cell levels to those of Wt animals within chronically-infected brains.

A number of cell surface molecules have been described as markers for Bregs, although complete elucidation of these regulatory cells remains to be achieved. It has been proposed that B-cells with immunoregulatory function may represent a transient stage of activation and maturation (54). In this study, we phenotyped Bregs based on the expression of specific cell surface markers that constituted reactivity to $CD19^+CD1d^{hi}CD5^+$. B-cells, Breg and B10 cells are known to regulate adaptive immune responses through multiple mechanisms which include: secretion of IL-10 (55) and promoting proliferation of $CD4^+Foxp3^+$ Tregs (52, 56), as well as through inhibitory B7 family molecules which promote Treg and IL-10 production (56). Previous studies have shown that IL-10 competent B-cells (B10 cells) are predominantly found within this Breg subset, particularly in the spleen (41).

It has been shown that responses of Bregs can be induced by stimulation with TLR4 and TLR9 ligands, as well as signaling through the B-cell receptor (BCR) (15, 57). Krug A., *et al* (58) reported that MCMV engages with TLR9 to induce dendritic and interferon-producing cell activation and enhance immune responses to infection. It is also possible that the Breg response observed in this study results from direct stimulation of B-cells by

MCMV or its antigens. Although a number of studies involving various infectious agents have demonstrated the expansion of Bregs in peripheral immune appendages, to our knowledge, this is the first demonstration of the chronic presence of Bregs within the brain following MCMV infection.

We previously demonstrated that $CD8^+$ T-cells control replication and persist within the brain even after active viral replication ceases (32, 59). In addition, our studies and others have shown that IFN-γ produced from infiltrating T-cells drives microglial activation (30, 60). Persistence of $CD8^+$ T-cells is particularly important because they constitute the major brain-infiltrating immune cell type during the chronic phase of infection; they are retained at a ratio of 3:1 to $CD4^+$ T-cells. In the present study, we observed that there were significantly higher numbers of $CD8^+$ T-cells present in the chronically-infected brain (i.e., 30 d p.i.) in the absence of B-cells. Conversely, we observed a lower frequency of $CD4^+$ and $CD4^+Foxp3^+$ T-cells than in Wt animals. Similar findings have been reported using an EAE model in which the authors noted that depletion of B-cells during disease development results in significant reduction in total $CD4^+$ T-cell, myelin oligodendrocyte glycoprotein (MOG)-specific T-effector, and Treg numbers within the CNS. However, these authors also state that before disease induction there was significant increase in the accumulation of all the above three cell types, suggesting that depletion of B-cells at specific stages of the disease may have had different outcomes on encephalitogenic T-cells (16).

Bregs have been shown to control macrophage-driven pro-inflammatory responses. Previous studies have revealed that B-cell depletion causes enhanced macrophage activation and cytokine production during *Listeria* infection (61). Similarly, in this study we reported increased activation of brain resident microglia as assessed by MHC class II expression perhaps in the context of reduced Treg presence and in turn insufficient control of $CD8^+$ T-cells influx. This increased activation of microglia could be due to enhanced production of IFN-γ. IFN-γ has been shown to drive microglial activation (60). There was also a small increase in the expression levels of CD40 and CD86 molecules on the microglial cells at 30 d p.i., which confirmed increased activation of these cells in B-cell deficient animals. Our *in vitro* studies provide a mechanistic explanation for the inhibition of microglial cell activation through B10 cell-produced IL-10. The data presented in this study are in agreement with findings that have demonstrated that B10 cells down-regulate macrophage activation following LPS stimulation (61).

Bregs have also been shown to promote conversion of $CD4^+$ T-cells into a regulatory T-cell phenotype. A recent study, using a collagen-induced arthritis (CIA) model, demonstrated that B10 cells promoted Treg conversion when co-cultured with naïve $CD4^+$ T-cells (62). T-cell plasticity has been well recognized, and many factors are known to influence plasticity including: cellular conditions, transcriptional circuitry, and chromatin modifications (63). Our *in vitro* studies using B10:$CD4^+$ T-cell co-cultures found that these cells increased Treg proliferation that is demonstrated by Ki67 expression by $Foxp3^+$ cells. Utilizing both *in vivo* and *in vitro* approaches a recent elegant study by Ray A. *et al* (52) has shown that Treg proliferation in the presence of B-cells is attributed to the interaction of glucocorticoid-induced TNFR family-related protein (GITR) with its ligand, the study also demonstrated that Treg proliferation was IL-10 independent. Although Tregs are not the main focus of this

study, their role in controlling neuroinflammation is well established. Likewise, the presence of B10 cells during chronic phase of the disease could be beneficial as they are capable of driving proliferation of Tregs and in turn may aid in controlling excessive neuroinflammation.

In animal models of allergic disease, Amu and colleagues (64) suggested that Bregs may have a more systemic effect on Treg expansion. Other studies demonstrated that IL-10-producing B10 cells function to down-regulate autoimmunity and allergic disorders by inducing Tregs (15, 64, 65). These findings can be extended to our chronic viral brain infection model. In particular, adoptive transfer of B-cells in this animal model resulted in enhanced amounts of Tregs, to a level exhibited by B-cell-sufficient animals. Thus, our data demonstrate that transfer of B-cells inhibits the exacerbated neuroimmune responses that are observed in B-cell-deficient mice.

Results generated from these studies demonstrate that the absence of B-cells leads to exacerbated microglial cell- and T-cell-mediated neuroinflammation following viral infection, suggesting the importance of these cells in controlling chronic and persistent immune activation in the brain. This knowledge may be useful in the development of therapeutic applications to modulate chronic neuroimmune activation and its associated neuropathology.

Acknowledgments

Funding: This project was supported by Award Number R01NS-038836 from the National Institute of Neurological Disorders and Stroke.

References

1. Gonzalez-Scarano F, Martin-Garcia J. The neuropathogenesis of AIDS. Nat Rev Immunol. 2005; 5:69–81. [PubMed: 15630430]
2. McGavern DB, Kang SS. Illuminating viral infections in the nervous system. Nat Rev Immunol. 2011; 11:318–329. [PubMed: 21508982]
3. Goverman J. Autoimmune T cell responses in the central nervous system. Nat Rev Immunol. 2009; 9:393–407. [PubMed: 19444307]
4. Kivisakk P, Imitola J, Rasmussen S, Elyaman W, Zhu B, Ransohoff RM, Khoury SJ. Localizing central nervous system immune surveillance: meningeal antigen-presenting cells activate T cells during experimental autoimmune encephalomyelitis. Ann Neurol. 2009; 65:457–469. [PubMed: 18496841]
5. Hu S, Sheng WS, Schachtele SJ, Lokensgard JR. Reactive oxygen species drive herpes simplex virus (HSV)-1-induced proinflammatory cytokine production by murine microglia. J Neuroinflammation. 2011; 8:123. [PubMed: 21943001]
6. Aravalli RN, Hu S, Rowen TN, Palmquist JM, Lokensgard JR. Cutting edge: TLR2-mediated proinflammatory cytokine and chemokine production by microglial cells in response to herpes simplex virus. J Immunol. 2005; 175:4189–4193. [PubMed: 16177057]
7. Phares TW, Disano KD, Hinton DR, Hwang M, Zajac AJ, Stohlman SA, Bergmann CC. IL-21 optimizes T cell and humoral responses in the central nervous system during viral encephalitis. J Neuroimmunol. 2013; 263:43–54. [PubMed: 23992866]
8. Ransohoff RM, Brown MA. Innate immunity in the central nervous system. J Clin Invest. 2012; 122:1164–1171. [PubMed: 22466658]

9. Stewart BS, Demarest VL, Wong SJ, Green S, Bernard KA. Persistence of virus-specific immune responses in the central nervous system of mice after West Nile virus infection. BMC Immunol. 2011; 12:6. [PubMed: 21251256]
10. Anghelina D, Zhao J, Trandem K, Perlman S. Role of regulatory T cells in coronavirus-induced acute encephalitis. Virology. 2009; 385:358–367. [PubMed: 19141357]
11. Reuter D, Sparwasser T, Hunig T, Schneider-Schaulies J. Foxp3+ regulatory T cells control persistence of viral CNS infection. PLoS One. 2012; 7:e33989. [PubMed: 22448284]
12. Graham JB, Da Costa A, Lund JM. Regulatory T cells shape the resident memory T cell response to virus infection in the tissues. J Immunol. 2014; 192:683–690. [PubMed: 24337378]
13. Howard M, O'Garra A. Biological properties of interleukin 10. Immunol Today. 1992; 13:198–200. [PubMed: 1385707]
14. Marques CP, Hu S, Sheng W, Cheeran MC, Cox D, Lokensgard JR. Interleukin-10 attenuates production of HSV-induced inflammatory mediators by human microglia. Glia. 2004; 47:358–366. [PubMed: 15293233]
15. Yanaba K, Bouaziz JD, Haas KM, Poe JC, Fujimoto M, Tedder TF. A regulatory B cell subset with a unique CD1dhiCD5+ phenotype controls T cell-dependent inflammatory responses. Immunity. 2008; 28:639–650. [PubMed: 18482568]
16. Matsushita T, Yanaba K, Bouaziz JD, Fujimoto M, Tedder TF. Regulatory B cells inhibit EAE initiation in mice while other B cells promote disease progression. J Clin Invest. 2008; 118:3420–3430. [PubMed: 18802481]
17. Matsushita T, Horikawa M, Iwata Y, Tedder TF. Regulatory B cells (B10 cells) and regulatory T cells have independent roles in controlling experimental autoimmune encephalomyelitis initiation and late-phase immunopathogenesis. J Immunol. 2010; 185:2240–2252. [PubMed: 20624940]
18. Mauri C, Bosma A. Immune regulatory function of B cells. Annu Rev Immunol. 2012; 30:221–241. [PubMed: 22224776]
19. Fillatreau S, Sweenie CH, McGeachy MJ, Gray D, Anderton SM. B cells regulate autoimmunity by provision of IL-10. Nat Immunol. 2002; 3:944–950. [PubMed: 12244307]
20. Schioppa T, Moore R, Thompson RG, Rosser EC, Kulbe H, Nedospasov S, Mauri C, Coussens LM, Balkwill FR. B regulatory cells and the tumor-promoting actions of TNF-alpha during squamous carcinogenesis. Proc Natl Acad Sci U S A. 2011; 108:10662–10667. [PubMed: 21670304]
21. Ding Q, Yeung M, Camirand G, Zeng Q, Akiba H, Yagita H, Chalasani G, Sayegh MH, Najafian N, Rothstein DM. Regulatory B cells are identified by expression of TIM-1 and can be induced through TIM-1 ligation to promote tolerance in mice. J Clin Invest. 2011; 121:3645–3656. [PubMed: 21821911]
22. Goenka R, Parent MA, Elzer PH, Baldwin CL. B cell-deficient mice display markedly enhanced resistance to the intracellular bacterium Brucella abortus. J Infect Dis. 2011; 203:1136–1146. [PubMed: 21451002]
23. Neves P, Lampropoulou V, Calderon-Gomez E, Roch T, Stervbo U, Shen P, Kuhl AA, Loddenkemper C, Haury M, Nedospasov SA, Kaufmann SH, Steinhoff U, Calado DP, Fillatreau S. Signaling via the MyD88 adaptor protein in B cells suppresses protective immunity during Salmonella typhimurium infection. Immunity. 2010; 33:777–790. [PubMed: 21093317]
24. Gray M, Miles K, Salter D, Gray D, Savill J. Apoptotic cells protect mice from autoimmune inflammation by the induction of regulatory B cells. Proc Natl Acad Sci U S A. 2007; 104:14080–14085. [PubMed: 17715067]
25. Haas KM, Watanabe R, Matsushita T, Nakashima H, Ishiura N, Okochi H, Fujimoto M, Tedder TF. Protective and pathogenic roles for B cells during systemic autoimmunity in NZB/W F1 mice. J Immunol. 2010; 184:4789–4800. [PubMed: 20368280]
26. Yanaba K, Bouaziz JD, Matsushita T, Tsubata T, Tedder TF. The development and function of regulatory B cells expressing IL-10 (B10 cells) requires antigen receptor diversity and TLR signals. J Immunol. 2009; 182:7459–7472. [PubMed: 19494269]
27. Watanabe R, Ishiura N, Nakashima H, Kuwano Y, Okochi H, Tamaki K, Sato S, Tedder TF, Fujimoto M. Regulatory B cells (B10 cells) have a suppressive role in murine lupus: CD19 and

B10 cell deficiency exacerbates systemic autoimmunity. J Immunol. 2010; 184:4801–4809. [PubMed: 20368271]

28. Kamanaka M, Kim ST, Wan YY, Sutterwala FS, Lara-Tejero M, Galan JE, Harhaj E, Flavell RA. Expression of interleukin-10 in intestinal lymphocytes detected by an interleukin-10 reporter knockin tiger mouse. Immunity. 2006; 25:941–952. [PubMed: 17137799]
29. Maseda D, Smith SH, DiLillo DJ, Bryant JM, Candando KM, Weaver CT, Tedder TF. Regulatory B10 cells differentiate into antibody-secreting cells after transient IL-10 production in vivo. J Immunol. 2012; 188:1036–1048. [PubMed: 22198952]
30. Mutnal MB, Hu S, Little MR, Lokensgard JR. Memory T cells persisting in the brain following MCMV infection induce long-term microglial activation via interferon-gamma. J Neurovirol. 2011; 17:424–437. [PubMed: 21800103]
31. Mutnal MB, Hu S, Lokensgard JR. Persistent humoral immune responses in the CNS limit recovery of reactivated murine cytomegalovirus. PLoS One. 2012; 7:e33143. [PubMed: 22412996]
32. Cheeran MC, Gekker G, Hu S, Palmquist JM, Lokensgard JR. T cell-mediated restriction of intracerebral murine cytomegalovirus infection displays dependence upon perforin but not interferon-gamma. J Neurovirol. 2005; 11:274–280. [PubMed: 16036807]
33. Stoddart CA, Cardin RD, Boname JM, Manning WC, Abenes GB, Mocarski ES. Peripheral blood mononuclear phagocytes mediate dissemination of murine cytomegalovirus. J Virol. 1994; 68:6243–6253. [PubMed: 8083964]
34. Nanton MR, Way SS, Shlomchik MJ, McSorley SJ. Cutting edge: B cells are essential for protective immunity against Salmonella independent of antibody secretion. J Immunol. 2012; 189:5503–5507. [PubMed: 23150714]
35. Chen J, Trounstine M, Alt FW, Young F, Kurahara C, Loring JF, Huszar D. Immunoglobulin gene rearrangement in B cell deficient mice generated by targeted deletion of the JH locus. Int Immunol. 1993; 5:647–656. [PubMed: 8347558]
36. Cheeran MC, Gekker G, Hu S, Min X, Cox D, Lokensgard JR. Intracerebral infection with murine cytomegalovirus induces CXCL10 and is restricted by adoptive transfer of splenocytes. J Neurovirol. 2004; 10:152–162. [PubMed: 15204920]
37. Cheeran MC, Hu S, Palmquist JM, Bakken T, Gekker G, Lokensgard JR. Dysregulated interferon-gamma responses during lethal cytomegalovirus brain infection of IL-10-deficient mice. Virus Res. 2007; 130:96–102. [PubMed: 17624463]
38. Levine B, Hardwick JM, Trapp BD, Crawford TO, Bollinger RC, Griffin DE. Antibody-mediated clearance of alphavirus infection from neurons. Science. 1991; 254:856–860. [PubMed: 1658936]
39. Marten NW, Stohlman SA, Zhou J, Bergmann CC. Kinetics of virus-specific CD8+-T-cell expansion and trafficking following central nervous system infection. J Virol. 2003; 77:2775–2778. [PubMed: 12552021]
40. Mutnal MB, Cheeran MC, Hu S, Little MR, Lokensgard JR. Excess neutrophil infiltration during cytomegalovirus brain infection of interleukin-10-deficient mice. J Neuroimmunol. 2010; 227:101–110. [PubMed: 20655600]
41. Yoshizaki A, Miyagaki T, DiLillo DJ, Matsushita T, Horikawa M, Kountikov EI, Spolski R, Poe JC, Leonard WJ, Tedder TF. Regulatory B cells control T-cell autoimmunity through IL-21-dependent cognate interactions. Nature. 2012; 491:264–268. [PubMed: 23064231]
42. Fantini MC, Dominitzki S, Rizzo A, Neurath MF, Becker C. In vitro generation of CD4+ CD25+ regulatory cells from murine naive T cells. Nat Protoc. 2007; 2:1789–1794. [PubMed: 17641646]
43. Chao CC, Hu S, Sheng WS, Bu D, Bukrinsky MI, Peterson PK. Cytokine-stimulated astrocytes damage human neurons via a nitric oxide mechanism. Glia. 1996; 16:276–284. [PubMed: 8833198]
44. Suzumura A, Mezitis SG, Gonatas NK, Silberberg DH. MHC antigen expression on bulk isolated macrophage-microglia from newborn mouse brain: induction of Ia antigen expression by gamma-interferon. J Neuroimmunol. 1987; 15:263–278. [PubMed: 3110208]
45. Giulian D, Baker TJ, Shih LC, Lachman LB. Interleukin 1 of the central nervous system is produced by ameboid microglia. J Exp Med. 1986; 164:594–604. [PubMed: 3487617]

46. Hassan NF, Rifat S, Campbell DE, McCawley LJ, Douglas SD. Isolation and flow cytometric characterization of newborn mouse brain-derived microglia maintained in vitro. J Leukoc Biol. 1991; 50:86–92. [PubMed: 2056249]
47. Cheeran MC, Lokensgard JR, Schleiss MR. Neuropathogenesis of congenital cytomegalovirus infection: disease mechanisms and prospects for intervention. Clin Microbiol Rev. 2009; 22:99–126. Table of Contents. [PubMed: 19136436]
48. Zelinskyy G, Werner T, Dittmer U. Natural regulatory T cells inhibit production of cytotoxic molecules in CD8+ T cells during low-level Friend retrovirus infection. Retrovirology. 2013; 10:109. [PubMed: 24156479]
49. Sungur CM, Tang-Feldman YJ, Ames E, Alvarez M, Chen M, Longo DL, Pomeroy C, Murphy WJ. Murine natural killer cell licensing and regulation by T regulatory cells in viral responses. Proc Natl Acad Sci U S A. 2013; 110:7401–7406. [PubMed: 23589894]
50. Qureshi MH, Garvy BA, Pomeroy C, Inayat MS, Oakley OR. A murine model of dual infection with cytomegalovirus and Pneumocystis carinii: effects of virus-induced immunomodulation on disease progression. Virus Res. 2005; 114:35–44. [PubMed: 16002171]
51. Fiorentino DF, Zlotnik A, Mosmann TR, Howard M, O'Garra A. IL-10 inhibits cytokine production by activated macrophages. J Immunol. 1991; 147:3815–3822. [PubMed: 1940369]
52. Ray A, Basu S, Williams CB, Salzman NH, Dittel BN. A novel IL-10-independent regulatory role for B cells in suppressing autoimmunity by maintenance of regulatory T cells via GITR ligand. J Immunol. 2012; 188:3188–3198. [PubMed: 22368274]
53. Liu Y, Chen Y, Li Z, Han Y, Sun Y, Wang Q, Liu B, Su Z. Role of IL-10-producing regulatory B cells in control of cerebral malaria in Plasmodium berghei infected mice. Eur J Immunol. 2013; 43(11):2907–2918. [PubMed: 23893352]
54. Gray D, Gray M. What are regulatory B cells? Eur J Immunol. 2010; 40:2677–2679. [PubMed: 21038464]
55. DiLillo DJ, Matsushita T, Tedder TF. B10 cells and regulatory B cells balance immune responses during inflammation, autoimmunity, and cancer. Ann N Y Acad Sci. 2010; 1183:38–57. [PubMed: 20146707]
56. Mann MK, Maresz K, Shriver LP, Tan Y, Dittel BN. B cell regulation of CD4+CD25+ T regulatory cells and IL-10 via B7 is essential for recovery from experimental autoimmune encephalomyelitis. J Immunol. 2007; 178:3447–3456. [PubMed: 17339439]
57. Miles K, Heaney J, Sibinska Z, Salter D, Savill J, Gray D, Gray M. A tolerogenic role for Toll-like receptor 9 is revealed by B-cell interaction with DNA complexes expressed on apoptotic cells. Proc Natl Acad Sci U S A. 2012; 109:887–892. [PubMed: 22207622]
58. Krug A, French AR, Barchet W, Fischer JA, Dzionek A, Pingel JT, Orihuela MM, Akira S, Yokoyama WM, Colonna M. TLR9-dependent recognition of MCMV by IPC and DC generates coordinated cytokine responses that activate antiviral NK cell function. Immunity. 2004; 21:107–119. [PubMed: 15345224]
59. Marques CP, Cheeran MC, Palmquist JM, Hu S, Urban SL, Lokensgard JR. Prolonged microglial cell activation and lymphocyte infiltration following experimental herpes encephalitis. J Immunol. 2008; 181:6417–6426. [PubMed: 18941232]
60. Ponomarev ED, Shriver LP, Maresz K, Dittel BN. Microglial cell activation and proliferation precedes the onset of CNS autoimmunity. J Neurosci Res. 2005; 81:374–389. [PubMed: 15959904]
61. Horikawa M, Weimer ET, DiLillo DJ, Venturi GM, Spolski R, Leonard WJ, Heise MT, Tedder TF. Regulatory B cell (B10 Cell) expansion during Listeria infection governs innate and cellular immune responses in mice. J Immunol. 2013; 190:1158–1168. [PubMed: 23275601]
62. Yang M, Deng J, Liu Y, Ko KH, Wang X, Jiao Z, Wang S, Hua Z, Sun L, Srivastava G, Lau CS, Cao X, Lu L. IL-10-producing regulatory B10 cells ameliorate collagen-induced arthritis via suppressing Th17 cell generation. Am J Pathol. 2012; 180:2375–2385. [PubMed: 22538089]
63. Murphy KM, Stockinger B. Effector T cell plasticity: flexibility in the face of changing circumstances. Nat Immunol. 2010; 11:674–680. [PubMed: 20644573]

64. Amu S, Saunders SP, Kronenberg M, Mangan NE, Atzberger A, Fallon PG. Regulatory B cells prevent and reverse allergic airway inflammation via FoxP3-positive T regulatory cells in a murine model. J Allergy Clin Immunol. 2010; 125:1114–1124. e1118. [PubMed: 20304473]

65. Hussaarts L, van der Vlugt LE, Yazdanbakhsh M, Smits HH. Regulatory B-cell induction by helminths: implications for allergic disease. J Allergy Clin Immunol. 2011; 128:733–739. [PubMed: 21684587]

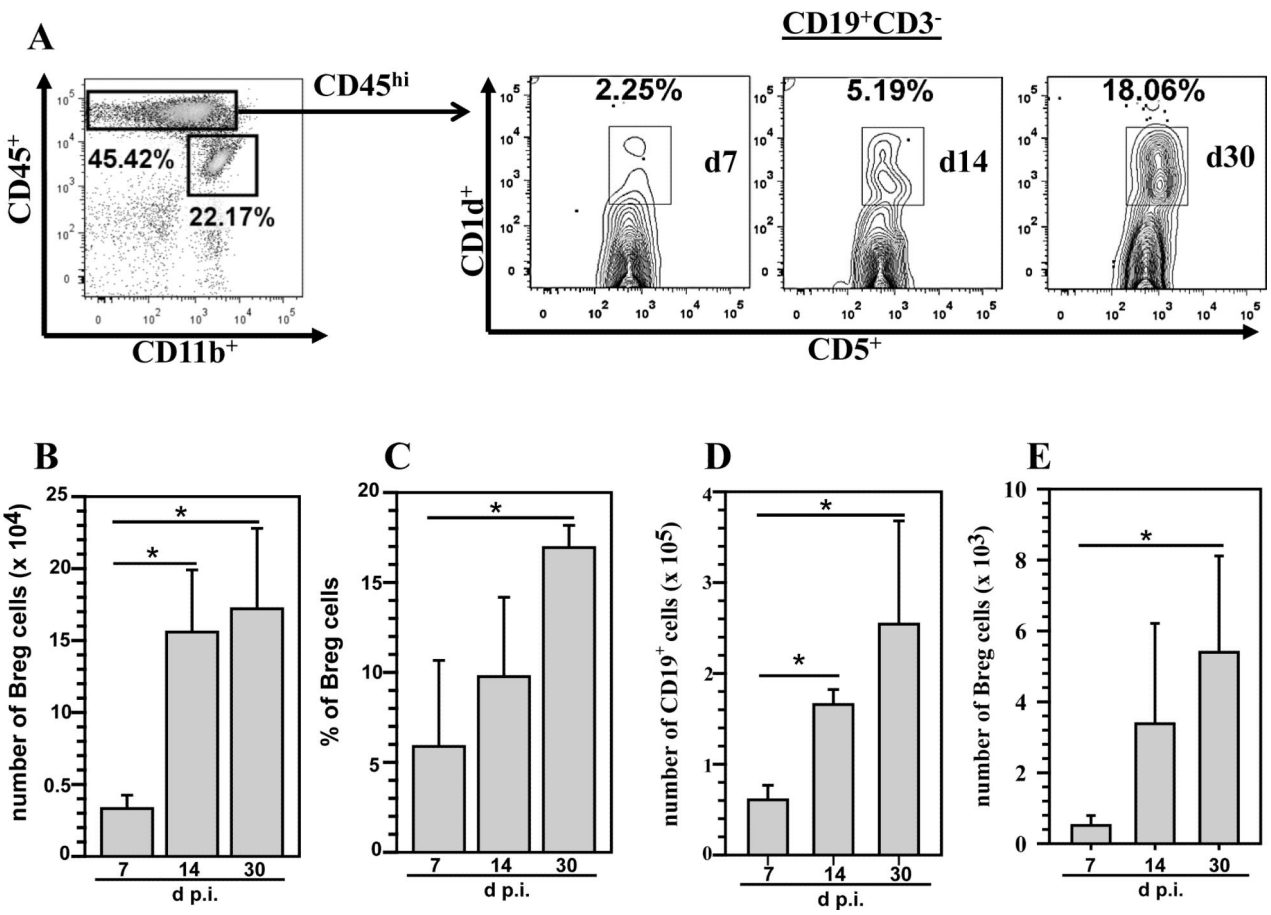

Figure 1. B regulatory cells (Bregs) persist in the brain during chronic viral infection

Single cell suspensions of brain tissue obtained from MCMV-infected mice (3–5 animals) per time point were banded on a 70% Percoll cushion. Brain leukocytes were collected and labeled with PE-Cy5-conjugated Abs specific for CD45, AF700-labeled anti-CD11b Abs, and APC-Cy7 anti-CD19 Abs; and analyzed using flow cytometry. Breg cells were identified within the $CD45^{hi}$ cell population by using a Breg staining kit (BioLegend, San Diego, CA). The data obtained were processed using FlowJo software. **A.** Representative flow cytometric plots show the percentages of $CD45^{hi}CD19^{+}CD1d^{hi}CD5^{+}$ Breg cells within the infiltrating $CD45^{hi}CD3^{-}$ population obtained from infected brains at 7, 14, and 30 d p.i. **B.** $CD19^{+}$ $CD1d^{hi}Cd5^{+}$ Abs were used to determine the total number of Breg cells within the infiltrating $CD45^{hi}CD3^{-}$ population. Data shown are mean (±SEM) absolute number of infiltrating cells pooled from 3 independent experiments (n = 3–5). **C.** Percentage of Bregs within the infiltrating $CD45^{hi}CD3^{-}$ cell population at indicated time points from three independent experiments are shown (n = 3–5). *$P < 0.05$, 30 d p.i. versus 7 and 14 d p.i. **D.** Absolute numbers of $CD19^{+}$ cells determined from the total CD45hi population including $CD3^{+}$ cells. **E.** Absolute numbers of CD1dhi$CD5^{+}$ cells determined within the infiltrating CD45hi population including $CD3^{+}$ cells. *P <0.05, 30 d p.i. versus 7 and or 14 d p.i.

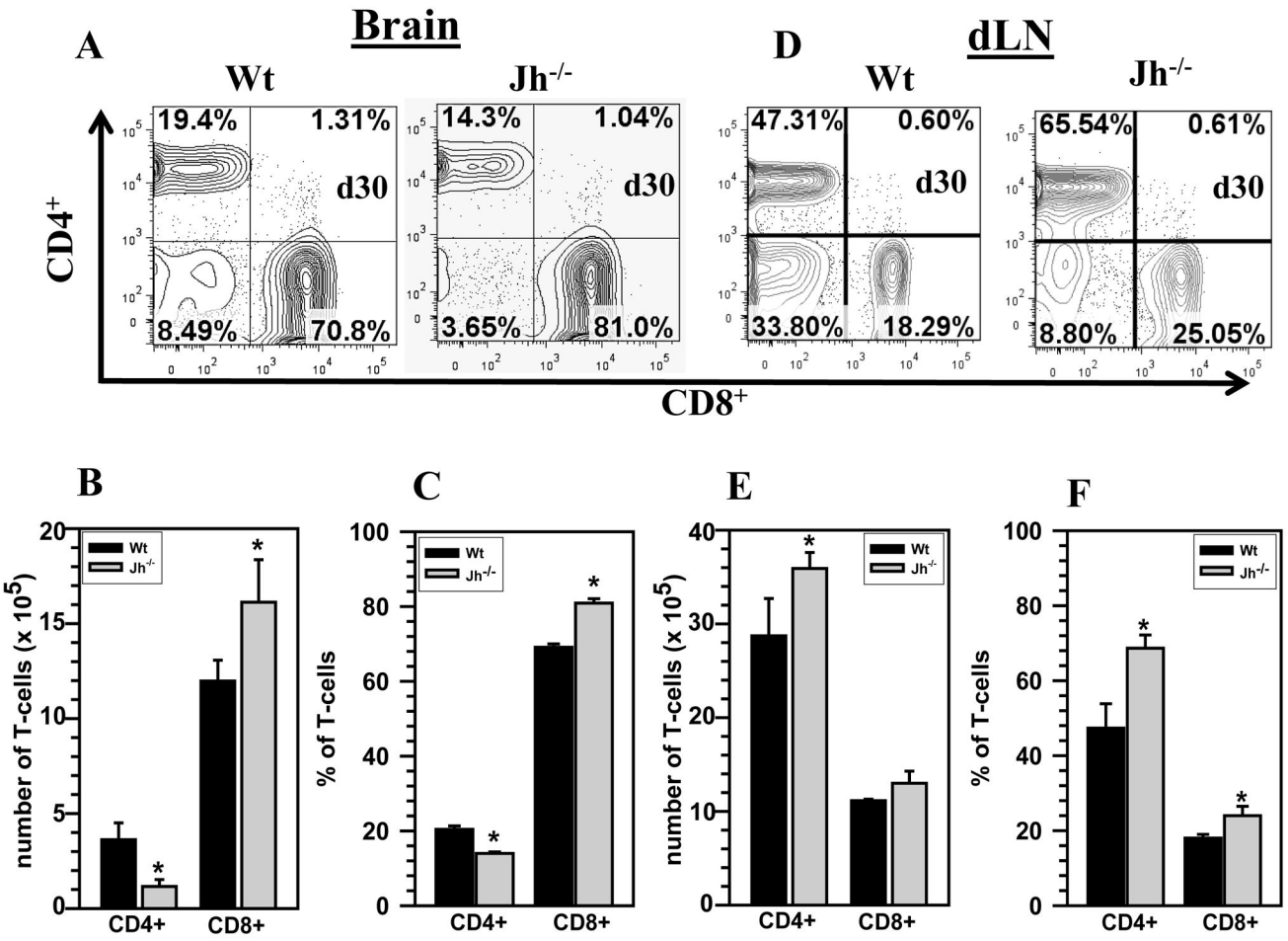

Figure 2. T-cell responses are altered within the brains of B-cell deficient mice

Wt and B-cell deficient ($Jh^{-/-}$) mice were infected with MCMV and brain-infiltrating leukocytes were collected at 30 d p.i. and labeled with PE-Cy5-conjugated Abs specific for CD45, AF700-labeled anti-CD11b, eFlour 450-CD4, and PE-Cy7-CD8; and analyzed using flow cytometry. **A.** Representative contour plots showing the percentages of $CD4^+$ and $CD8^+$ T-cells within the brain-infiltrating $CD45^{hi}$ population at 30 d p.i. are shown. **B.** Specific fluorescent-tagged mAB were used to stain $CD4^+$ and $CD8^+$ cells and determine total T-cell numbers within the infiltrating $CD45^{hi}$ population. Data shown are mean (±SEM) absolute number of infiltrating cells pooled from 3 independent experiments (n=5). **C**. The percentage of $CD4^+$ and $CD8^+$ T-cell subsets at 30 d p.i. from three independent experiments are shown (n=5). **D**. Representative contour plots from dLN of Wt and $Jh^{-/-}$ mice infected with MCMV at 30 d p.i. **E.** The absolute number of $CD4^+$ and $CD8^+$ T-cells from the dLN of Wt and $Jh^{-/-}$ animals was determined and presented as pooled data from 3 independent experiments (n=5). **F.** The percentage of $CD4^+$ and $CD8^+$ T-cell subsets in dLN from three independent experiments are shown (n=5). $^*P < 0.05$ *versus infected Wt.*

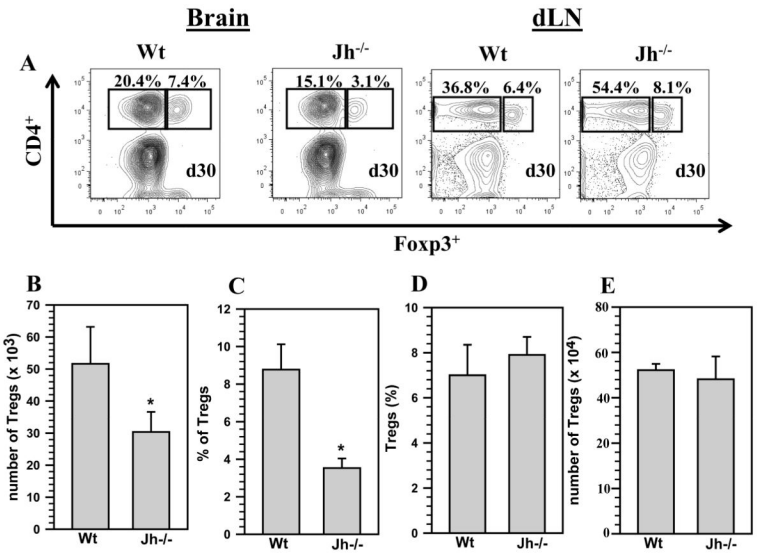

Figure 3. Absence of B-cells leads to decreased numbers of regulatory T-cells within the brain

Wt and Jh$^{-/-}$ mice were infected with MCMV and brain tissue samples were obtained at 30 d p.i. Brain leukocytes were collected and labeled with PE-Cy5-conjugated Abs specific for CD45, AF700-labeled anti-CD11b, eFlour450-CD4, and FITC-Foxp3; and analyzed using flow cytometry. **A.** Representative contour plots show the percentages of CD4^{+}Foxp3^{+} Tregs within the infiltrating CD45^{hi} population in the infected brains at 30 d p.i. Also, representative contour plots are shown from dLN of Wt and Jh−/− mice collected at 30 d p.i. **B.** FITC labeled anti-Foxp3 Abs were used to determine the total number of Tregs within the infiltrating CD45^{hi} population (n=5). Data shown are mean (±SEM) absolute number of infiltrating cells pooled from 3 independent experiments. **C.** The percentage of CD4^{+}Foxp3^{+} Tregs within CD45^{hi} population from three independent experiments are also shown (n=5). **D.** The absolute number of CD4^{+}Foxp3^{+} T-cells was also determined from the dLN of Wt and Jh$^{-/-}$ animals and presented as pooled data from 3 independent experiments (n=5). **E.** The percentage of CD4^{+}Foxp3^{+} T-cell subsets in dLN from three independent experiments are shown (n=5). **P <0.05 versus infected Wt.*

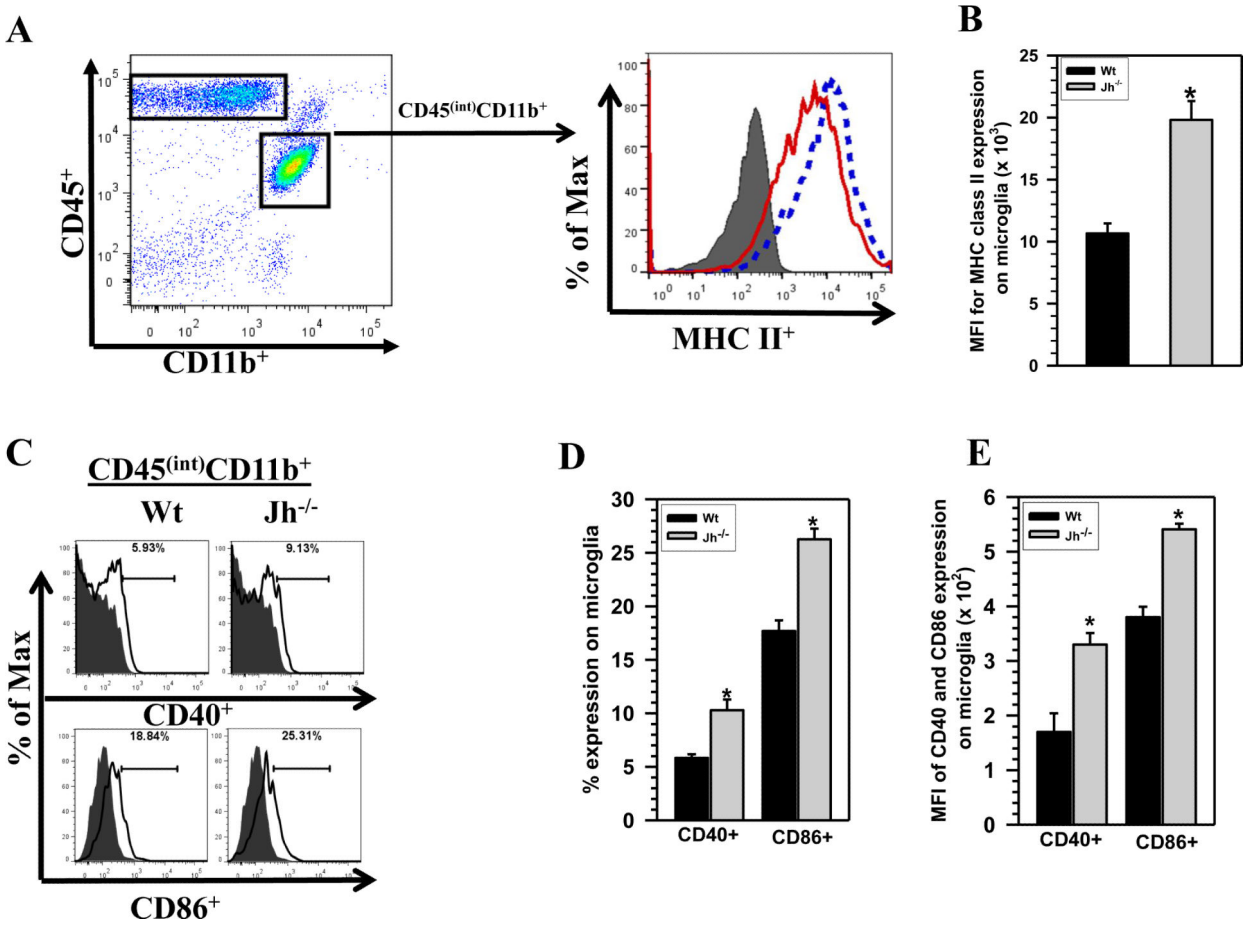

Figure 4. B-cell deficient mice display increased levels of chronic microglial cell activation

Brain mononuclear cells isolated from animals at 30 d p.i. were stained using anti-CD45, anti-CD11b, and anti-MHC-II surface marker Abs. **A.** Up-regulation of MHC class II on the $CD45^{int}CD11b^{+}$ resident microglial cells from Wt and $Jh^{-/-}$ mice in response to viral brain infection was compared. An overlay of histograms from isotype (grey, shaded), Wt (red, solid line) mice and from $Jh^{-/-}$ (blue, dotted line) animals is shown. **B**. Data presented show mean fluorescent intensity (MFI) of MHC-II binding to microglia from Wt versus $Jh^{-/-}$ mice (n=5). **C**. Representative histogram overlays for CD40 and CD86 expression on microglial cells isolated from Wt and $Jh^{-/-}$ mice are shown. The overlay of histograms from isotype (grey, shaded) and specific marker (solid line) are shown for the respective groups. **D.** Data presented in the bar graph shows percentage of CD40 and CD86 expression on microglia from Wt versus $Jh^{-/-}$ mice (n=5). *$p < 0.01$ versus infected Wt for* Fig 4B and *p < 0.05 versus infected Wt for Fig 4D. **E.** Mean fluorescent intensity (MFI) of CD40 and CD86 expression on microglia obtained from Wt versus $Jh^{-/-}$ mice. *p < 0.01 versus infected Wt for Fig 4B; and *p < 0.05 versus infected Wt for Fig 4D and E.

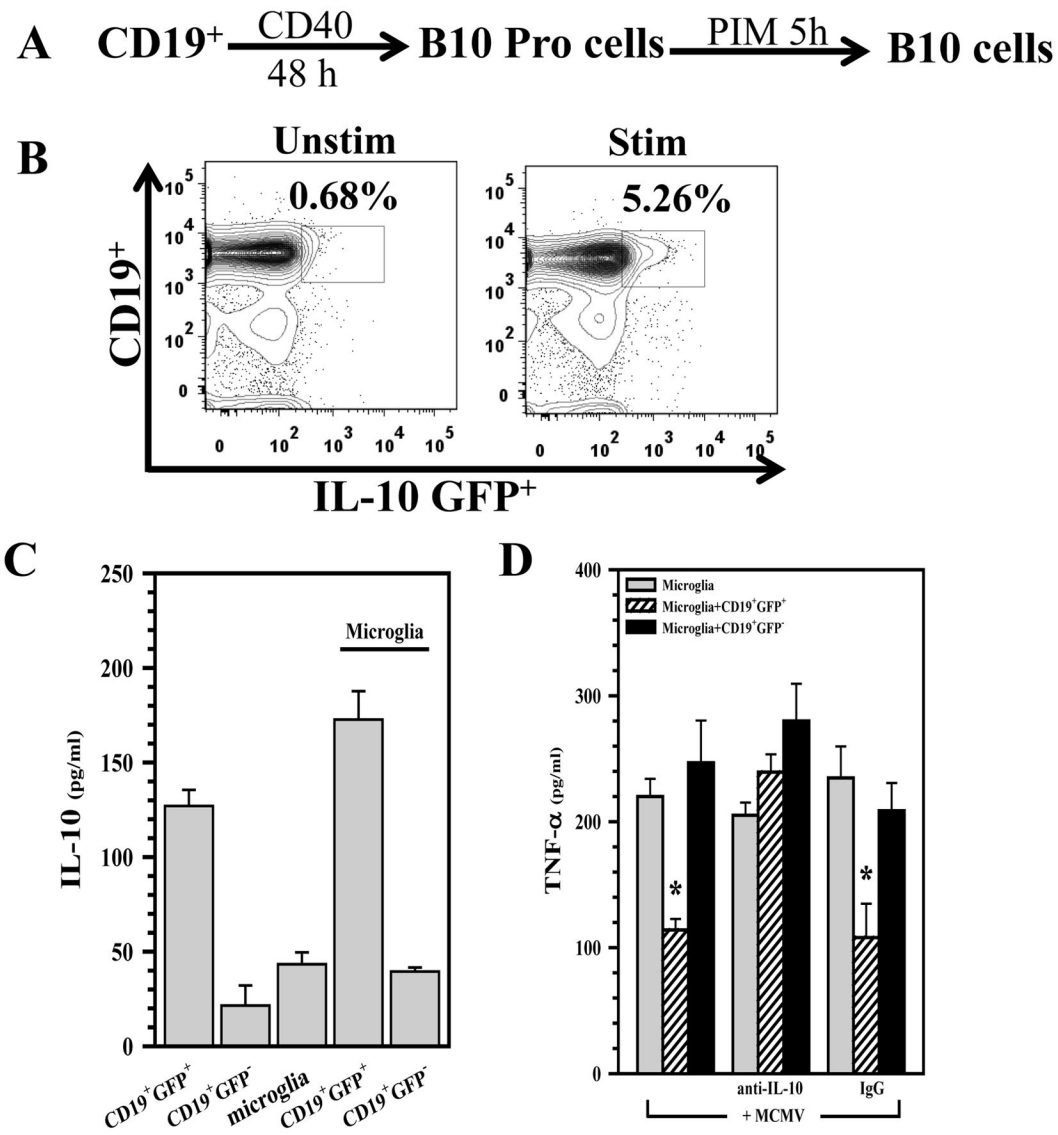

Figure 5. Induced B10 cells modulate microglial cell activation

A. Splenic CD19$^+$ B-cells from IL-10-GFP knock-in mice were cultured with agonistic CD40 mAB (1 μg/ml, eBioscience San Diego, CA) for 48 h. For the last 5 h, cells were treated with LPS (10 μg/ml, Sigma), PMA (50 ng/ml, eBioscience San Diego, CA), ionomycin (100 ng/ml, eBioscience San Diego, CA), and monensin (PIM) (eBioscience San Diego, CA) for 5 h to induce IL-10-producing B10 cells. **B.** Representative flow cytometry contour plots showing IL-10 induction in CD19$^+$ cells that were stimulated with the above protocol. **C.** The induced B10 cells were then added to purified cultures of primary murine microglia (1:1 ratio) and IL-10 production in these co-cultures was assessed using ELISA. **D.** CD19$^+$IL-10-GFP$^+$ B10, as well as CD19$^+$IL-10-GFP$^-$, cells were enriched using FACS and then added to primary microglial cell cultures. Co-cultures were incubated for 5 h, followed by stimulation with MCMV (MOI=5), and assessment of TNF-α production (at 24h) using ELISA. **p < 0.05 CD19$^+$GFP$^+$ versus microglia alone; *p < 0.05 anti-IL-10 versus IgG isotype*

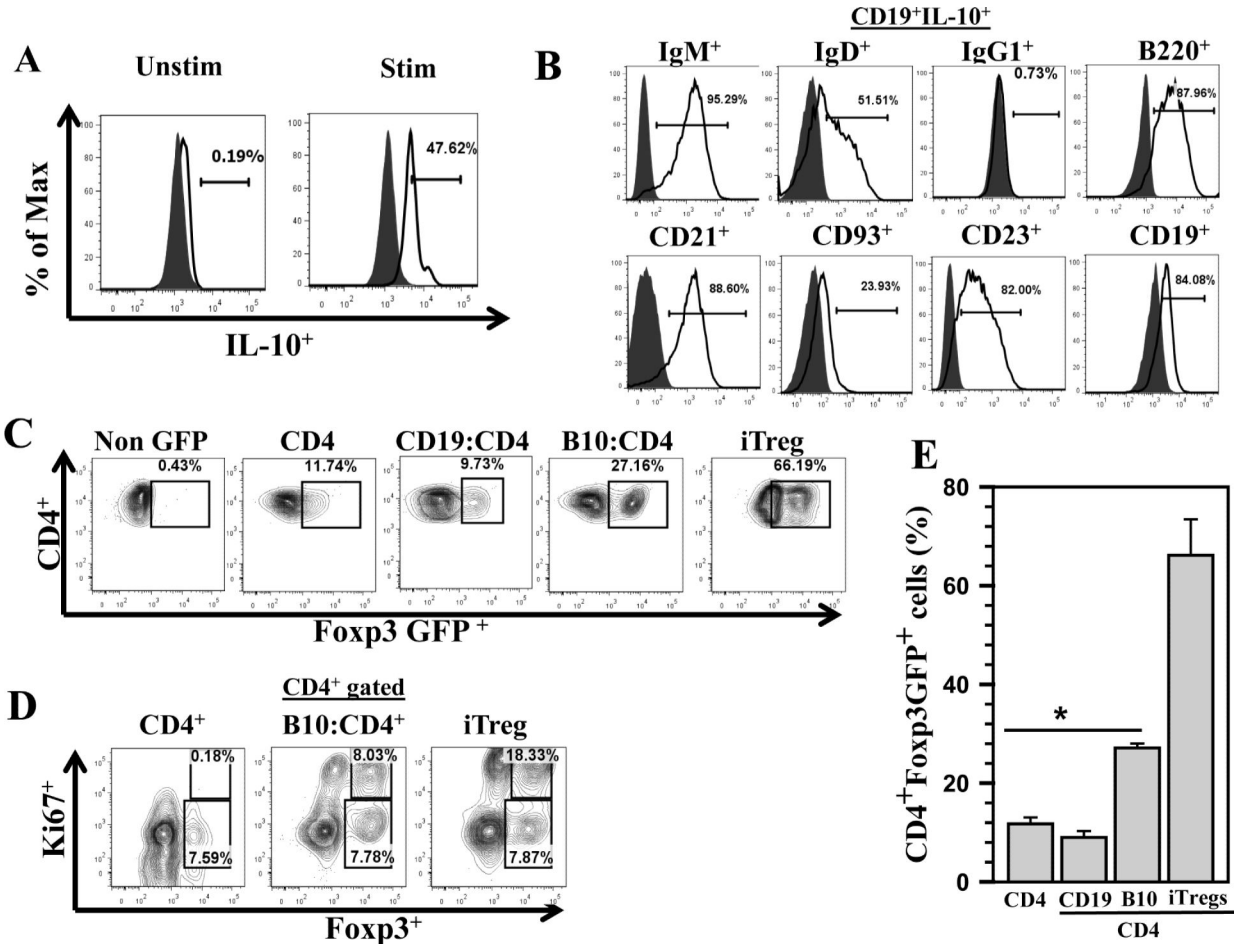

Figure 6. Induced B10 cells promote proliferation of Foxp3$^+$ Treg cells

Regulatory B10 cells were prepared from CD19$^+$ cells as described and CD4$^+$ T-cells were isolated from MHC-matched donors, Foxp3^{EGFP+}, using a negative selection kit. Induced B10 cells were added to the CD4$^+$ T-cell cultures at a 1:1 ratio. The co-cultures were then incubated for 72 h and Foxp3^{EGFP+} expression within the CD4$^+$ T-cell population was assessed by flow cytometry for GFP expression to assess Treg phenotype. **A.** Flow cytometry histogram overlays show staining for isotype (grey, shaded) and intracellular IL-10 (solid line) levels in the induced B10 cells. **B.** B10 cells generated through this protocol were subjected to phenotyping to determine expression of various B-cell surface markers. Representative histogram overlays, gated from the CD19$^+$IL-10$^+$ population, which include isotype (grey, shaded) and specific markers (solid line) are shown. **C.** Representative flow cytometry contour plots of Foxp3^{EGFP+} within the CD4$^+$ T-cell population are shown: non-GFP, CD4$^+$ T-cells only (CD4), total B-cells with CD4$^+$ T-cells (CD19$^+$:CD4$^+$), and induced B10 cells with CD4$^+$ T-cells (B10:CD4$^+$); along with a standard protocol used to generate *in vitro* Treg cells as a positive control (iTregs). **D**. Representative flow cytometry analysis of Foxp3$^+$Ki67$^+$ expression within CD4$^+$ T-cells co-cultured with CD4 only, CD4:B10 and positive control iTreg are shown. **E.** The percentages of CD4$^+$Foxp3$^+$ in the various treatment groups from three independent experiments are shown. **P <0.01 versus CD4$^+$T-cells alone and total B-cells+CD4$^+$ T-cells*

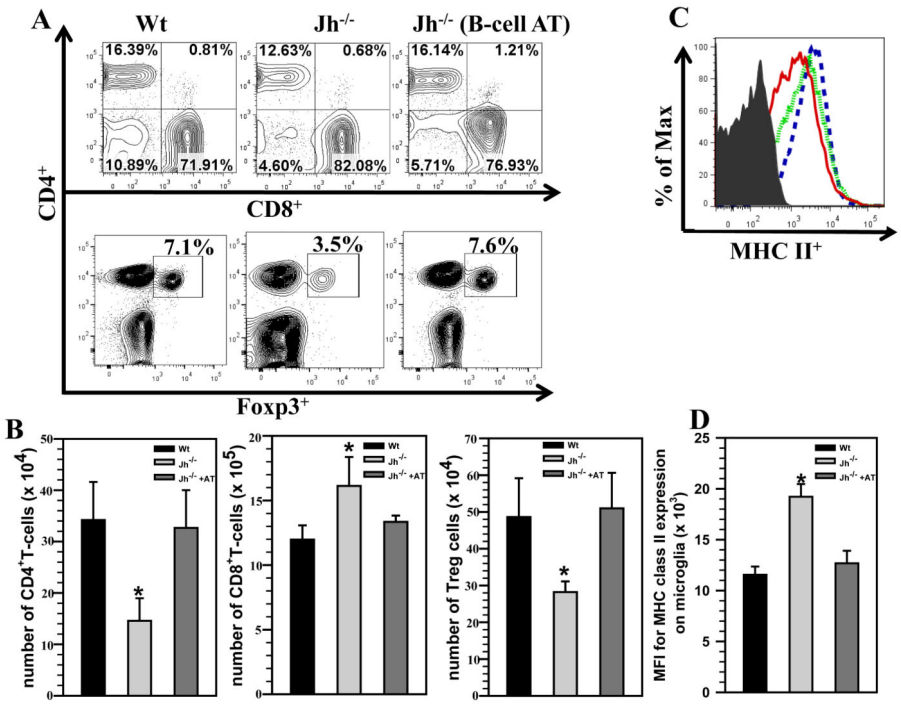

Figure 7. B-cell replenishment restores T-cell levels within chronically-infected brains

MCMV-primed splenocytes and lymph node cells from donor BALB/c mice were enriched for $CD19^+$ cells using negative selection. These B-cells were then adoptively transferred via tail vein injection into MHC-matched $Jh^{-/-}$ recipients 1 d prior to the infection with MCMV. Wt and $Jh^{-/-}$ mice served as appropriate controls and brain tissue samples were obtained from each group at 30 d p.i. Brain leukocytes were collected and labeled with PE-Cy5-conjugated Abs specific for PE-Cy5-labeled anti-CD45, AF700-labeled anti-CD11b, eFlour450-labeled anti-CD4, PE-Cy7-labeled anti-CD8, FITC-labeled anti-Foxp3 and APC-Cy7-labeled anti-MHC II and analyzed using flow cytometry. **A.** Representative contour plots showing the percentages of $CD4^+$, $CD8^+$ (upper panel), and $CD4^+Foxp3^+$ T-cells (lower panel) in the infiltrating $CD45^{hi}$ population within the infected brains from each group. **B.** The absolute numbers of $CD4^+$, $CD8^+$ and $CD4^+Foxp3^+$ T-cells were also determined among the brain-infiltrating $CD45^{hi}$ cells from Wt, $Jh^{-/-}$, and $Jh^{-/-}$ with B-cell AT animals. Pooled data obtained from 3 independent experiments are presented (n=5 per group). *$p < 0.05$ $Jh^{-/-}$+*AT versus* $Jh^{-/-}$ **C.** Histogram overlays from isotype (grey, shaded), Wt (red, solid), $Jh^{-/-}$ (blue, dashed), and $Jh^{-/-}$ mice that received $CD19^+$ cells (green, dotted) are shown for MHC class II up-regulation on $CD45^{int}CD11b^+$ resident microglia. **D**. Data presented show mean fluorescent intensity (MFI) of MHC-II binding from Wt, $Jh^{-/-}$ and $Jh^{-/-}$+AT mice (n=5 per group).*$p < 0.01$ $Jh^{-/-}$+*AT versus* $Jh^{-/-}$